Title
A HIGH CURRENT PULSED ION SOURCE FOR METALLIC IONS

Author
Gavin, B.

Publication Date
1981-03-01

Peer reviewed

Lawrence Berkeley Laboratory
UNIVERSITY OF CALIFORNIA

Accelerator & Fusion Research Division

Presented at the IEEE 1981 Particle Accelerator
Conference, Washington, D.C., March 11-13, 1981

A HIGH CURRENT PULSED ION SOURCE FOR METALLIC IONS

B. Gavin, S. Abbott, R. MacGill, R. Sorensen,
J. Staples, and R. Thatcher

March 1981

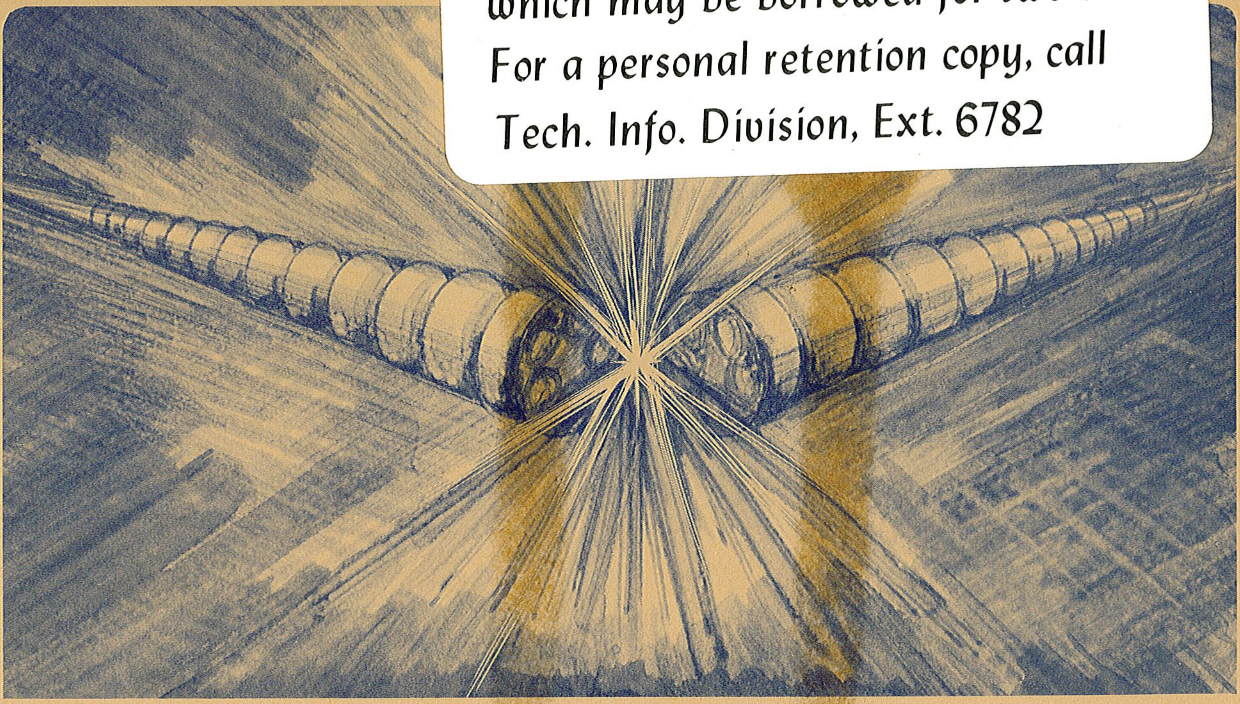

Prepared for the U.S. Department of Energy under Contract W-7405-ENG-48

LBL-11706 (preprint)

A HIGH CURRENT PULSED ION SOURCE FOR METALLIC IONS*

B. Gavin, S. Abbott, R. MacGill, R. Sorensen, J. Staples, R. Thatcher**

Summary

A new sputter-ion PIG source and magnet system, optimized for intermediate charge states, q/A of 0.02-0.03, is described. This source will be used with the new Wideroe-based injector for the SuperHILAC. Pulsed electrical currents of several emA of heavy metal ions have been produced in a normalized emittance area of .05π cm-mr. The source system is comprised of two electrically separate anode chambers, one in operation and one spare, which can be selected by remote control. The entire source head is small and quickly removable.

Introduction

This report is divided into two parts: the results taken with the SuperHILAC Heavy Ion Source Test-stand (SHIST) followed by a description with performance data of the magnet and source for use in ABEL, the third injector of the SuperHILAC. Ions produced are typically $U^{5+(6+)}$, $Au^{4+(5+)}$, Xe^{3+}, Ca^{3+}, Nb^{2+}, and Ar^{2+}, usually at 36 pulses/sec., 15%. An approximate acceptance of 0.05π cm-mr (norm) was postulated for accelerator beam lines. Source and associated beam lines were assigned dimensions with excess phase space.

Test Stand Description

Fundamental parameters for the ABEL source and magnet were determined with a heated cathode-type PIG source, kindly loaned to us by GSI at Darmstadt. The 30.5 cm gap SHIST magnet can analyze the source output through a 180° bend into an internal traveling cup (ρ=8-41 cm), or through a 109° bend into an external beam line (ρ=27 cm). This magnet is equipped with edge shims for field correction, and is of sufficient size to analyze low charge state heavy ions. Field measurements were made for use with an orbit tracking code, ORBIT, written to calculate off-midplane field components and plot trajectories without space charge. The external beam line includes two sets of computer controlled slits for the usual emittance plots in the radial (xx') and axial (zz') planes.

Test Stand Results

For those charge states examined with the 180° configuration, beam intensity was found to increase with increasing field over the range of 3-5.2 kGauss. It was observed that at higher fields support gas flows could be lowered, accounting for a small increase in metallic ion intensity. Over this range,

Ion Examined:	Xe^{3+}	Xe^{7+}	Au^{5+}
Approximate Increase:	1.6X	3.5X	1.9X

Above 5.2 kGauss, Au^{5+} yield dropped ~10% at 6.2 kGauss. A thorough testing procedure was not followed, principally because of scheduling demands.

The SHIST extraction system consists of a single lens accelerating gap. Power supplies limit beam potential drop to ~24 kV maximum. However, the ABEL source and supplies were specified to operate up to 35 kV given a considered future source development program. For this reason, the ABEL PIG source will operate at 5 kGauss and 20 kV for U^{5+} extraction with satisfactory performance over a range, referred to already, from 4.4-6.0 kGauss.

Calorimeter measurements of total ion output for conditions to be expected with ABEL show emission limited fluxes of ~350 mA/cm^2 with argon. The square root mass scaling appears to apply for other elements. Orbit verification, emittance measurements, source slit dimensioning, and electrode sizing were examined using the 109° analysis configuration.

Aluminum dee plates were used above and below the 109° orbit to supply neutralizing electrons to the beam plasma. Various slit geometries were tested. The "GANIL-type" slit appeared superior. This 0.8 x 20 mm slit was extended in length to 45 mm as was the sputter electrode. While measured emittances increased, the beam intensity within the .05π cm-mr accelerator acceptance window also increased significantly. Table 1 gives beam intensities within this window for xx' and zz' phase space.

Table 1

Ion	Slit	ARC I	Current (ZZ')	% AREA	Current (XX')	% AREA
Xe^{3+}_{136}	20 mm	3.8	2.8 emA	80	2.75 emA	95
	45 mm	3.2	4.9 emA	73	4.6 emA	71

Lengthening the slit, then, increased beam brightness at this selected emittance, 1.7X for xenon in both planes. The 45 mm zz' .05π slit emittance contour shape was altered, and does represent a larger fraction of beam parallel to the median plane.

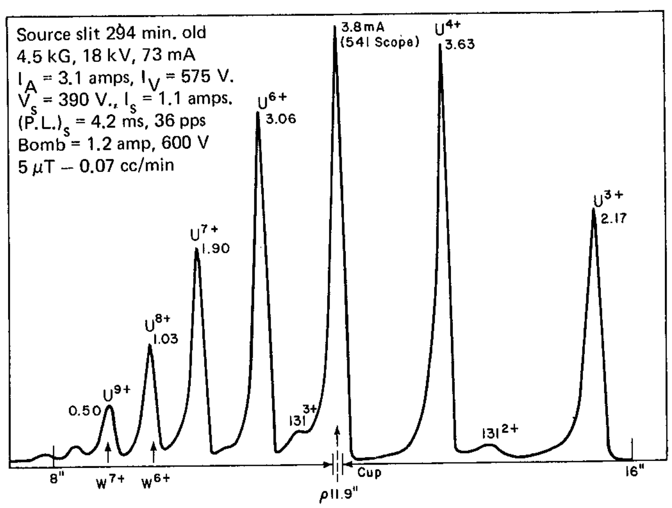

XBL 812-168

Figure 1. Ion current vs. ρ(radius). Modified GANIL slit, 1.1 x 45 mm; U/Xe; source age: 13 hrs.; cup width: .63 cm.

The increased sputter electrode length reduces support gas flow requirements substantially (~.07 cc/min, xenon/uranium). Figure 1 draws attention to the modest support gas flow in the SHIST 180° U spectrum. This spectrum is for a U^{5+} tune at 15% duty factor (D.F.), an average charge ~4.2, slit age ~5 hrs., and uranium use rate of 10 mgm/min., i.e. ~1.1 cc/min (at STP); U beam flux ~34 mA/cm^2. High use rates of sputter material are all too readily obtained with indiscriminate tuning.

When optimizing this source for these low charge to

*Work supported by the U.S. Dept. of Energy under Contract W-7405-ENG-48.
**Lawrence Berkeley Laboratory, University of California, Berkeley, CA 94720.

mass ions, the exit slit will become constricted quite rapidly, reducing beam output. Figure 2 shows characteristic beam attenuation over a 27 hr. period. The gold electrode loss rate averages 13.8 mg/min and the gold build up rate on the inside of the exit slit was ~9.7 mg/min. The rate of slit closure will increase at greater duty factor or higher arc power levels than selected for use in figure 1.

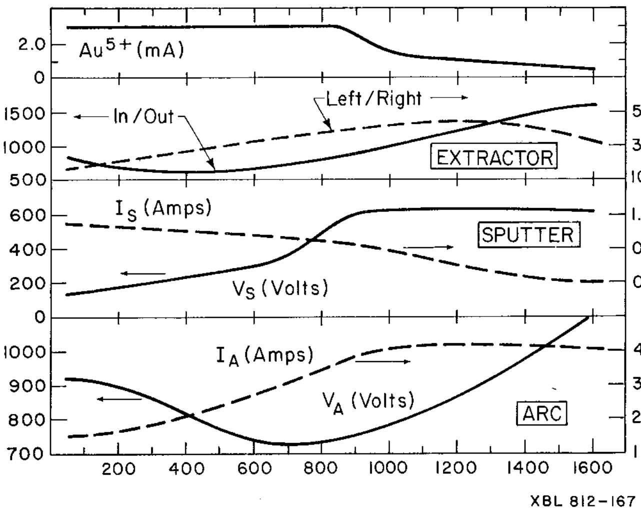

Figure 2. Source parameters vs time (min). Au^{5+} ion beam limited to 3 mA maximum, arc current limited to 4 amp maximum, duty factor: 15%.

Another electrode, the dynode, has been added to the SHIST source and, also, an additional 'sputter' supply so as to reduce, or possibly eliminate, slit closure. The dynode replaces the anode body in the vicinity of the sputter electrode and includes the exit slit, which is now operated at dynode potential. By biasing this electrode, deposited material is removed by back-sputtering to the original electrode, either during normal extraction time or at a later time. Small negative potentials (< 10 V) between dynode and anode during beam pulsing further optimizes ion output. Initial testing, not yet complete, shows that by selecting an appropriate bias voltage and pulse length for clean up, the gold build up rate may be reduced essentially to zero. However, the extractor blade wear rate does increase sufficiently to limit source yield, just as slit closure did. Nevertheless, integrated beam output over normal source life is increased ~25%. The ABEL terminal electronics will include a gated supply for the dynode; the extractor wear problem is expected to be overcome. Typical dynode I/V settings are: during beam acceleration: (4.5 msec), 0.5 A, -3 v, and clean up time: (1.5 msec) 0.8 A, -370 v. The arc pulse length under these conditions is extended and the consequent effect on total source output must be weighed against other considerations. It would appear that computer control of the clean up pulse may be quite suitable. Further study is called for, and will be expanded upon in a forthcoming LBL report.

ABEL Source and Magnet Description

The ABEL source is composed of two sets of source electrodes mounted on a common manifold at anode potential. Each set of electrodes comprises one complete source head interchangeable with the other as seen in figure 3. The dual-headed ABEL source is detachable from the support body of the source. Each source electrode is accurately located by short stub length tubes that simultaneously pass freon from manifold to electrode. The manifold then, serves to distribute freon to two source heads in parallel, i.e. to a total of 14 electrodes. The vacuum-to-freon seals use O-rings that are vacuum checked after source assembly and may be pronounced vacuum tight before the source heads are mounted to the main source body by the accelerator crew. See figure 3. Note that but two freon to vacuum O-rings need be inspected

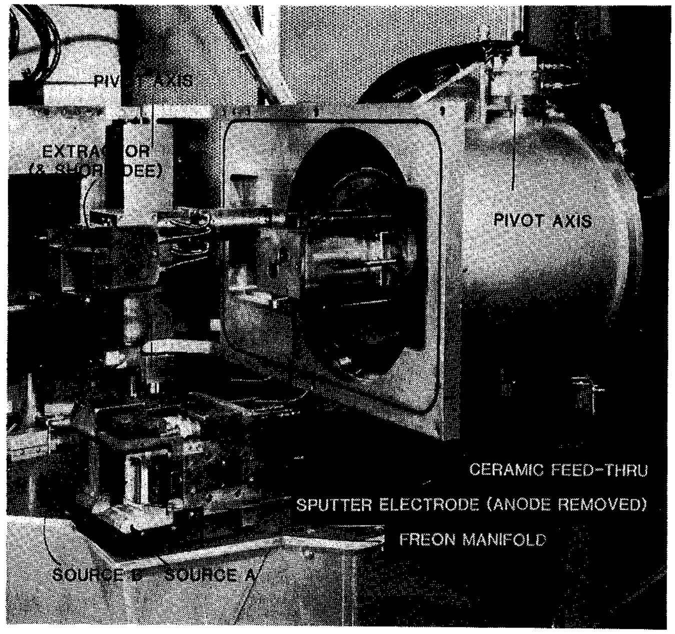

Figure 3. Source swung in open position. Dual head assembly below with one gas cap removed.

by the crew. A two lever overcenter cam lock is used to attach heads to main body. Freon flow rates for the dual head source measure 7.3 gpm (5 gpm with single head). Electrode electrical isolation is achieved with ceramic feed-throughs visible in figure 3. A series of 'Multilam' connectors must be slid along shafts when source heads are installed or removed. The main source body is then pivoted 7.4° about an axis located 40 cm from the magnet poles. Note that the main support insulator is under expansion from vacuum loading which reduces the length of source extension from source axis to vacuum wall without loss of the needed vacuum wall diameter. See figure 4. The extractor seen in figure 3 is driven either left or right and in or out with a hydraulic control system powered by air pressure. Linear potentiometers are used to generate accurate readouts of extractor position.

The ABEL magnet was designed with the use of the ORBIT code, tested previously with source location and beam direction matching in the SHIST magnet. This magnet allows for radial focusing of a beam with ±11° spread, through 142° and with ρ=28.4 cm. The magnetic gap is 17.7 cm, and the exit edge angle is 29°. Astigmatism in the radial plane is reduced by shimming the center rays (~±5°) with two shims, each with a frustum cross section, and each 2.7 cm tall (7.6 cm base) located after 68° of analysis*.

It should also be noted that this magnet will accommodate a multiple aperture diode LBL-type[2] source. This axial type source would utilize the ABEL magnet

*Later removal of these shims did, of course, alter the exit beam angle with regard to exit beam line, but had apparently a small effect on the xx' emittance plot distortion.

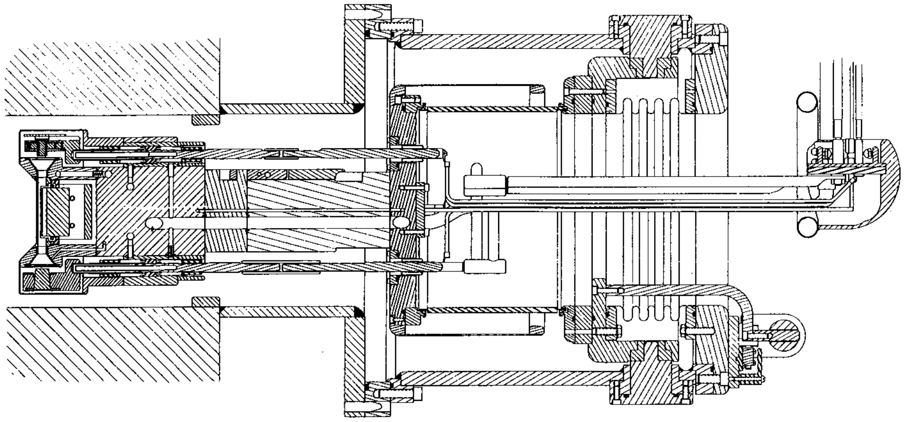

Figure 4. Elevation view of ABEL source; closed position.

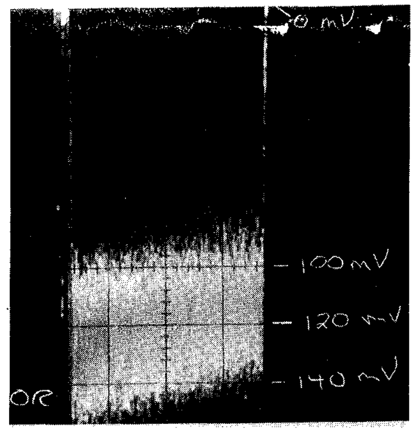

Figure 5. 2.4 emA Au^{4+}; across 50 ohm.

for separating ion species through a 69° analysis at two times the radius of curvature adopted for the PIG source. Entrance and exit beam line field clamps were modeled with MIRT[3], as were all shims, frustums, and edge shims for minimum field fall off and bowing at the source. The field was verified and corrected by median plane measurement.

Vacuum is provided by two 1 watt cryo CTI-72 pumps under each of the two beam lines, and a 10 watt CTI-1020 pump with cup valve located near the PIG ion beam, center of radius. Pumping speeds of 1500 l/sec with air were measured. A typical operating pressure of 10 μT is with recorded with xenon, the most frequently used support gas.

Results

The ORBIT code was used to predict a narrow waist in the radial plane, about 44 cm beyond the exit effective field boundary (EFB)*. Measurements showed the waist shifted an additional 19 cm (±10 cm, f(ion)) away from the magnet. This unforeseen shift may indicate that the beam is <100% neutralized. It has been observed that the dee separation (z plane) does in fact modify the brightness of the beam in the xx' plane. Dee plates with closer spacing appear to brighten the beam while also attenuating the beam. A compromise was reached by setting the dee divergent angle to 0.75°. Envelope convergence in the xx' plane is then measured at ±3.3° (±0.8°).

The axial plane emittance plots indicate envelopes converging gradually, ~1.5° (±0.8°). By selecting a number of rays originating at the exit slit with ORBIT, and plotting a zz' ellipse, and then comparing with the measured zz' plots; those beamlets that do match the brightest area, appear to be those that travel initially parallel to the median plane, with but a ±6° spread in the radial plane. Given an $\epsilon_n = .05\pi$, long slit lengths dictate the exclusion of rays from ±6° to <±11° in the radial plane. The absence of space charge forces with ORBIT should not alter this conclusion.

The ABEL terminal exit beam line will use collimation 46 cm from the exit EFB. At a normalized emittance of .05π, the beam will be ≤ 6 cm high and ≤ 3.6 cm wide. Figure 5 shows the degree of beam noise encountered with major components ~350 kHz.

Table 2 lists beam intensities at 80 cm from the EFB of the ABEL magnet. Arc currents vary from 2.5 to 4 amps, arc voltages from 500 to 1100 v, sputter voltages (currents) from 80 to 800 v (2 amp max). Extraction potentials are 20 kV, and slit size is 0.11 x 4.5 cm. The dee plates flare from entrance at the extractor to exit, with spacing from 5.5 to 8.5 cm. Charge states selected are optimized and indicated in the 'Ion Tuned' row.

*EFB is 3.5 cm from the pole edge.

Table 2

Ion Tuned	Ar^{1+}	Kr^{2+}_{86}	Nb^{2+}	Xe^{3+}_{136}	Au^{4+}	Au^{5+}	U^{5+}	U^{6+}	Au^{8+}
Total Intensity (emA)	9.0	9.0	6.0	5.0	4.6	3.1	3.6	3.0	.65
% Area, .05π XX'	50	60	62	67	86	89	83	68	60
% Area, .05π ZZ'	68	78	71	85	80	81	75	76	80
Corr. Intensity*	4.5/6.1	5.4/7.0	3.7/4.3	3.3/4.0	4.0/3.7	2.8/2.5	3.0/2.7	2.0/2.3	0.4/0.5

*Corrected intensity (emA) at $\epsilon_n = .05\pi$ cm-mr, expressed as that fraction of xx'/zz' space respectively.

Table 3 gives the charge state distribution of various elements with optimization indicated in the 'Ion Tuned' column. Magnetic fields are lowered below optimum values for tuning of the higher z ions. Ion currents are in emA, peak. Tungsten vapor from the PIG cathodes is efficiently ionized in the discharge to charge states 5+ to 10+, and will contaminate certain charge states reported. (E.g., Pb^{7+} is given an estimated value by virtue of being composed of ~14% W^{6+}.) Corrections were taken from prior data with the SHIST 109° analyzer and are included in the results of Table 3.

Table 3

Ion Tuned	ARC I/V	SPUT I/V	Gas	Extr	3+	4+	5+	6+	7+	8+	9+	Comments
U^{5+}	3.1 / 575	1.1 / 390	Xe	18	2.2	3.6	3.8	3.1	1.9	1.0	0.35	180°; Coll. = .63 cm
U^{5+}	3.6 / 750	1.8 / 200	Kr	20	–	2.8	3.6	3.3	2.4	1.2	0.4	ABEL; (10+) = 0.20
Pb^{5+}	2.5 / 1000	1.2 / 200	Xe	20	–	2.5	2.9	2.2	1.2	0.9	–	ABEL; (10+) ~0.1
Au^{8+}	2.7 / 1100	1.0 / 110	Kr^{86}	20	1.5	1.9	1.7	1.6	–	0.65	–	ABEL; (10+) = 0.13
Au^{4+}	2.5 / 1350	1.7 / 280	Xe	20	≤5.1	4.6	4.1	3.1	1.7	≤0.6	≤0.4	ABEL;
Au^{4+}	2.6 / 760	0.9 / 640	Xe	16	3.4	3.7	3.3	2.6	1.2	0.5	–	180°; Coll. = .63 cm
Xe^{3+}	2.8 / 630	–	Xe^{136}	20	4.7	2.7	2.4	1.8	1.5	1.0	0.3	ABEL; (2+) = 3.0
Xe^{3+}	2.6 / 1100	–	Xe	20	5.3	3.6	3.4	2.4	1.8	1.0	0.3	ABEL; (2+) = 4.7
Kr^{2+}	2.5 / 700	–	Kr^{86}	20	3.8	1.4	1.0	0.7	0.4	0.09	–	ABEL; (2+) = 6.2

References

[1] Private correspondence with L. Bex at GANIL, Caen, France.

[2] Chupp, W., et al. IEE Trans. Nucl. Sci. NS-26, 3, 3036 (1979).

[3] Halbach, K., Proc. 2 Inter. Conf. on Magnet Tech., Oxford, 1967.